






## Article

# Kvačekite, NiSbSe, a new selenide mineral from Bukov, Czech Republic

Petr Pauliš<sup>1,2</sup>, Zdeněk Dolníček<sup>1</sup>, Jiří Sejkora<sup>1</sup> , Ondřej Pour<sup>3</sup> , František Laufek<sup>3</sup>, Jana Ulmanová<sup>1</sup> and Anna Vymazalová<sup>3</sup> 

<sup>1</sup>Department of Mineralogy and Petrology, National Museum, Cirkusová 1740, 193 00, Prague 9, Czech Republic; <sup>2</sup>Smíškova 564, 284 01 Kutná Hora, Czech Republic; and <sup>3</sup>Czech Geological Survey, Geologická 6, 152 00 Prague 5, Czech Republic

### Abstract

Kvačekite is a new mineral species discovered in a sample collected from the now abandoned Bukov uranium mine, western Moravia, Czech Republic. It occurs as rare anhedral grains, up to 15 µm in size, associated with nickeltyrrellite, tyrrellite, berzelianite, hakite-(Zn), hakite-(Cd), eucairite, clausthalite, and gold in calcite gangue. In reflected light, kvačekite is white with a faint yellowish shade; bireflectance, pleochroism and anisotropy are absent. Internal reflections were not observed. Reflectance values for the four COM wavelengths for kvačekite in air [ $R$  (%) ( $\lambda$  in nm)] are: 54.9 (470); 53.5 (546); 52.6 (589); and 52.2 (650). The empirical formula, based on electron-microprobe analyses (EPMA), is  $(\text{Ni}_{0.95}\text{Cu}_{0.04}\text{Co}_{0.03})_{\Sigma 1.02}\text{Sb}_{1.00}(\text{Se}_{0.97}\text{S}_{0.01})_{\Sigma 0.98}$ . The ideal formula is NiSbSe, which requires (in wt.%) Ni 22.63, Sb 46.93, Se 30.44, total 100.00. Kvačekite is cubic,  $P2_13$ , with unit-cell parameters  $a = 6.09013(13)$  Å,  $V = 225.881(15)$  Å<sup>3</sup> and  $Z = 4$ . The strongest reflections in the X-ray powder diffraction pattern of synthetic kvačekite [ $d$ , Å ( $I$ )  $hkl$ ] are: 3.0458 (11) 200; 2.7242 (100) 201, 210; 2.4867 (71) 211; 1.8632(39) 311; 1.6277(29) 321, 312; and 1.3290 (13) 421. Given the similarity with ullmannite, NiSbS, the crystal structure was refined from the powder X-ray diffraction data starting from those atomic coordinates using the synthetic analogue of kvačekite. Its crystal structure is formed by corner-sharing  $[\text{NiSb}_3\text{Se}_3]$  octahedra which form a three-dimensional network. The identity of the natural kvačekite and synthetic cubic NiSbSe were confirmed by a study of their chemical composition, reflectance measurements, Raman spectroscopy and electron back-scattered diffraction (EBSD) measurements on the mineral. Kvačekite is named after Milan Kvaček (1930–1993), a prominent Czech mineralogist. The mineral and its name have been approved by the Commission on New Minerals, Nomenclature and Classification of the International Mineralogical Association (IMA2023-095).

**Keywords:** kvačekite; new mineral; selenide; nickel; antimony; crystal structure; Bukov; Czech Republic

(Received 10 February 2024; accepted 16 April 2024; Accepted Manuscript published online: 25 April 2024)

### Introduction

The Bukov mine (Rožná–Olší uranium district, Czech Republic) represents the most significant selenide mineralisation in the Bohemian Massif in terms of size of the selenide (especially berzelianite and umangite) aggregates and their abundance (Kvaček, 1973, 1979). At present, seventeen selenide species are reported from the Bukov mine (e.g. <https://www.mindat.org/loc-757.html>), including descriptions of the new minerals bukovite (Johan and Kvaček, 1971) and sabatierite (Johan *et al.*, 1978). During the systematic investigation of selenides from the various occurrences of the Bohemian Massif, we identified a possible Se analogue of ullmannite in a Ni–Co rich selenide association from the Bukov mine. Thus, a crystal-chemical investigation was undertaken, which confirmed its identity with synthetic NiSbSe and led to the proposal of the new mineral species, kvačekite.

**Corresponding author:** Jiří Sejkora; Email: [jiri.sejkora@nm.cz](mailto:jiri.sejkora@nm.cz)

Associate Editor: Ian Graham

**Cite this article:** Pauliš P., Dolníček Z., Sejkora J., Pour O., Laufek F., Ulmanová J. and Vymazalová A. (2024) Kvačekite, NiSbSe, a new selenide mineral from Bukov, Czech Republic. *Mineralogical Magazine* 88, 565–575. <https://doi.org/10.1180/mgm.2024.32>

This new mineral and its name were approved by the Commission on New Minerals, Nomenclature and Classification of the International Mineralogical Association (IMA2023–095, Pauliš *et al.*, 2024). Kvačekite is named after Milan Kvaček (13. 2. 1930 to 21. 5. 1993), a Czech mineralogist and the author of the first comprehensive descriptions of selenides from western Moravia (Kvaček, 1973, 1979). Milan Kvaček is the author of over sixty publications in the fields of mineralogy, chemistry and geochemistry. He also co-operated closely with Zdeněk Johan from BRGM (Orléans) on the description of six new selenides from the Bohemian Massif – bukovite, fischesserite, hakite, permingeaitite, petrovicite and sabatierite. Its mineral symbol, in accord with Warr (2021), is Kvč. The holotype material (polished section) is deposited in the mineralogical collection of the Department of Mineralogy and Petrology of the National Museum, Prague, Czech Republic (catalogue number PIP 26/2023).

### Occurrence and mineral description

#### Occurrence

The new mineral was discovered in material from Milan Kvaček's research collection originating from the now abandoned Bukov

mine, located on the northeastern edge of the village of Bukov, 35 km southeast of Nové Město na Moravě, Vysočina Region, Czech Republic. The GPS coordinates of the type occurrence are 49°27'27.333"N, 16°13'43.224"E.

The Bukov mine is a part of the Rožná–Olší uranium ore district with a total mine production of 23,000 t U in the years 1957–2017 (Křibek *et al.*, 2009, 2022). This uranium ore district is an example of shear-zone hosted, late Variscan and post-Variscan hydrothermal mineralisation (Křibek *et al.*, 2009). Uranium mineralisation is bound to a system of NNW–SSE trending faults and zones of cataclases, which are hosted in high-grade metamorphic rocks with a Moldanubian Zone of the Bohemian Massif. Mineralised cataclases are 4–15 m thick and are traceable over a horizontal distance of 15 km. The mineralised zones strike 340–355° and dip WSW at angles of 45–70° (Křibek *et al.*, 2022). The host rocks mainly comprise gneisses and amphibolites, with small bodies of calc-silicate gneiss, marble, serpentinite and pyroxenite. The vein and disseminated mineralisation at Rožná comprises (1) pre-uranium quartz–sulfide and carbonate–sulfide mineralisation, (2) uranium, and (3) post-uranium carbonate–quartz–sulfide mineralisation (Křibek *et al.*, 2009, 2022). Uranium mineralisation in some carbonate veins is accompanied by selenides, which are generally slightly younger than the main uranium mineralisation (Křibek *et al.*, 2009). The most significant occurrences of selenides appear in calcite–uraninite veins in the upper levels (5<sup>th</sup> to 9th) of the Bukov mine in the underlying rocks of the uranium-bearing shear zone R1. Selenide mineralisation occurs in two distinct types. The first is represented by massive aggregates of predominant berzelianite up to several tens of cm in size, usually in association with Cu sulfides (chalcopyrite, bornite and chalcocite). The second type represents disseminated selenide grains, more rarely tiny veinlets, formed by diverse selenides of often microscopic dimensions (Kvaček, 1973, 1979). The full list of minerals (more than 110 species including 20 selenides) recorded from this area is given on <https://www.mindat.org/loc-27262.html>.

Kvačekite was identified in samples of white calcite gangue in association with nickeltyrrellite–tyrrellite, berzelianite, hakite-(Zn), hakite-(Cd), eucairite, clausthalite and gold.

### Experimental procedures

The small size of kvačekite grains and its intergrowths with other minerals prevented its extraction and isolation in an amount sufficient for the relevant crystallographic and structural investigations. Therefore, these measurements were performed on synthetic NiSbSe.

The synthetic NiSbSe phase was prepared using an evacuated silica glass tube method in the Laboratory of Experimental Mineralogy of the Czech Geological Survey in Prague. Nickel (99.999%), antimony (99.999%) and selenium (99.9999%) were used as starting materials for synthesis. The evacuated tube with its charge was sealed and annealed at 800°C. After cooling by a cold-water bath, the charge was ground into powder in acetone using an agate mortar and pestle, and thoroughly mixed to homogenise. The pulverised charge was sealed in an evacuated silica-glass tube again, and heated at 300°C for 3 months. The experimental product was then rapidly quenched in cold water. The size of obtained NiSbSe grains ranges from 2 to 20 µm.

### Physical and optical properties

Kvačekite occurs as anhedral grains up to 15 µm in size (Fig. 1), but usually only 2–5 µm across, in nickeltyrrellite, usually

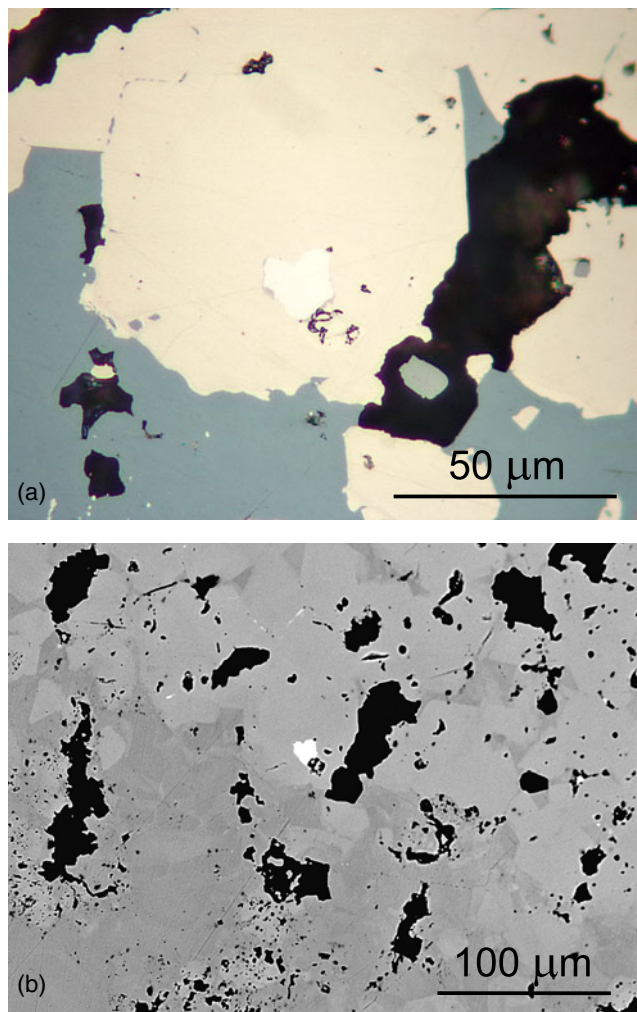


**Figure 1.** Kvačekite from Bukov: (a) reflected light image of kvačekite (white) associated with nickeltyrrellite (yellowish brown) and berzelianite (greenish blue); (b) back-scattered electron image (BSE) of kvačekite (white), nickeltyrrellite (light grey) and berzelianite (dark grey, zonal due to  $\text{SeS}_{-1}$  substitution). Holotype sample P1P 26/2023.

intergrown with hakite-(Zn) or clausthalite. Synthetic kvačekite is greyish white in colour with a grey streak and opaque in transmitted light; it has a metallic lustre. A cleavage was not observed; it is brittle with a conchoidal fracture. The calculated density for the empirical formula ( $Z = 4$ ) is 7.607 g·cm<sup>-3</sup>. Mohs hardness is assumed to be 5–6, in agreement with other members of the cobaltite group. In reflected light, kvačekite is white with a faint yellowish shade; bireflectance, pleochroism and anisotropy are absent. Internal reflections were not observed. Reflectance spectra for kvačekite and synthetic NiSbSe were measured in air with a TIDAS MSP400 spectrophotometer attached to a Leica microscope (100× objective) using a WTiC (Zeiss No. 370) standard, with a square sample measurement field of ca. 4 × 4 µm. The results for the 400–700 nm range are given in Table 1 and plotted in Fig. 2.

### Chemical composition

Chemical analyses of kvačekite from Bukov and synthetic NiSbSe were performed using a Cameca SX100 electron microprobe

**Table 1.** Reflectance values (%) for kvačekite and synthetic NiSbSe.<sup>a</sup>

$\lambda$ (nm)	R (%)		$\lambda$ (nm)	R (%)	
	kvačekite	NiSbSe		kvačekite	NiSbSe
400	53.7	53.6	560	53.2	52.8
420	54.8	54.5	580	52.8	52.4
440	55.0	54.4	<b>589</b>	<b>52.6</b>	<b>52.2</b>
460	55.0	54.1	600	52.4	52.1
<b>470</b>	<b>54.9</b>	<b>54.1</b>	620	52.3	51.8
480	54.8	54.1	640	52.2	51.8
500	54.5	53.8	<b>650</b>	<b>52.2</b>	<b>51.8</b>
520	54.1	53.5	660	52.2	51.8
540	53.6	53.1	680	52.2	52.0
<b>546</b>	<b>53.5</b>	<b>53.0</b>	700	52.4	52.2

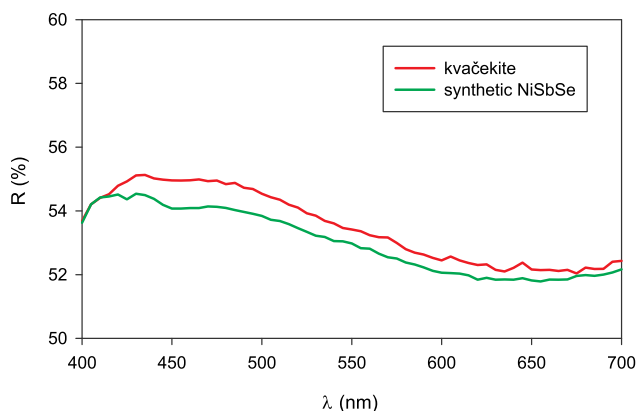
<sup>a</sup>The reference wavelengths required by the Commission on Ore Mineralogy (COM) are given in bold.

operating in wavelength-dispersive mode (25 kV, 20 nA and 0.7  $\mu\text{m}$  beam size). The following standards and X-ray lines were used to minimise line overlaps: Ag ( $\text{AgL}\alpha$ ), Au ( $\text{AuM}\alpha$ ),  $\text{Bi}_2\text{Se}_3$  ( $\text{BiM}\beta$ ), CdTe ( $\text{CdL}\alpha$ ), chalcopyrite ( $\text{CuK}\alpha$  and  $\text{SK}\alpha$ ), Co ( $\text{CoK}\alpha$ ), GaAs ( $\text{GaL}\alpha$ ), Ge ( $\text{GeL}\alpha$ ), HgTe ( $\text{HgM}\alpha$ ), Mo ( $\text{MoL}\alpha$ ), Ni ( $\text{NiK}\alpha$ ), NiAs ( $\text{AsL}\beta$ ), PbS ( $\text{PbM}\alpha$ ), PbSe ( $\text{SeL}\beta$ ), PbTe ( $\text{TeL}\alpha$ ), pyrite ( $\text{FeK}\alpha$ ),  $\text{Sb}_2\text{S}_3$  ( $\text{SbL}\alpha$ ), Sn ( $\text{SnL}\alpha$ ), Tl( $\text{Br,I}$ ) ( $\text{TlL}\alpha$ ) and ZnS ( $\text{ZnK}\alpha$ ). Peak counting times were 20 s for all elements, and 10 s for each background. Arsenic, Ag, Au, Bi, Cd, Fe, Ga, Ge, Hg, Mo, Pb, Sn, Te, Tl and Zn were all found to be below the detection limits (0.02–0.15 wt.%). Raw intensities were converted to the concentrations of elements using the automatic ‘PAP’ (Pouchou and Pichoir, 1985) matrix-correction procedure.

Analytical data for kvačekite from Bukov (17 analyses) and synthetic NiSbSe (6 analyses) are given in Table 2. On the basis of 3 atoms per formula unit (apfu), the empirical chemical formula of kvačekite is  $(\text{Ni}_{0.95}\text{Cu}_{0.04}\text{Co}_{0.03})_{\Sigma 1.02}\text{Sb}_{1.00}(\text{Se}_{0.97}\text{S}_{0.01})_{\Sigma 0.98}$  and  $\text{Ni}_{1.00}\text{Sb}_{1.02}\text{Se}_{0.98}$  for synthetic NiSbSe. The ideal formula is NiSbSe, which requires Ni 22.63, Sb 46.93 and Se 30.44, a total of 100.00 wt.%.

### Raman spectroscopy

The Raman spectra of kvačekite from Bukov and synthetic NiSbSe were collected in the range 40–4000  $\text{cm}^{-1}$  using a DXR dispersive Raman Spectrometer (Thermo Scientific) mounted on a confocal Olympus microscope. The Raman signal was excited by an unpolarised green 532 nm solid state, diode pumped laser and

**Figure 2.** Reflectance curve for kvačekite from Bukov compared with data for synthetic NiSbSe.**Table 2.** EPMA chemical data (wt.%) for kvačekite from Bukov and synthetic NiSbSe.

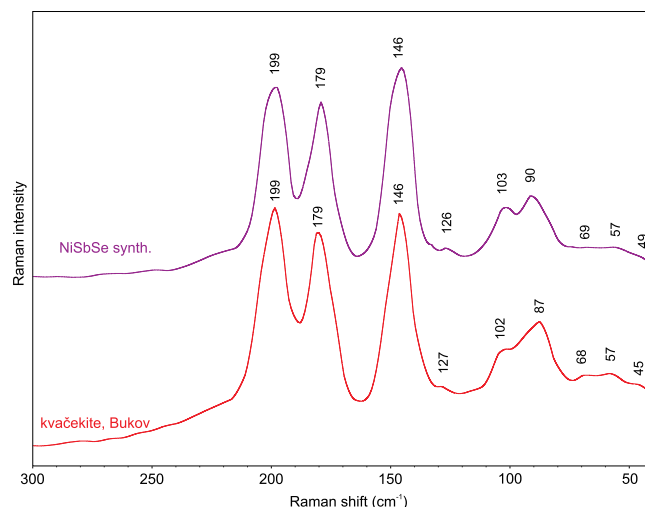
Constituent	Kvačekite from Bukov ( $n = 17$ )			Synthetic NiSbSe ( $n = 6$ )		
	Mean	Range	( $\sigma$ )	Mean	Range	( $\sigma$ )
Ni	21.60	20.63–22.08	0.37	22.41	20.80–23.57	0.99
Co	0.69	0.47–1.04	0.15			
Cu	1.06	0.69–2.56	0.47			
Sb	47.08	46.29–47.61	0.30	47.96	47.33–48.47	0.47
Se	29.69	29.13–30.15	0.32	29.62	28.88–30.59	0.61
S	0.14	0.05–0.23	0.05			
Total	100.26			99.98		

( $\sigma$ ) – estimated standard deviation;  $n$  = number of spot analyses.

detected by a CCD detector. The experimental parameters were: 100 $\times$  objective, 10 s exposure time, 100 exposures, 50  $\mu\text{m}$  slit spectrograph aperture and 1.5 mW laser power level. The eventual thermal damage of the measured points was excluded by visual inspection of the excited surface after measurement, by observation of possible decay of spectral features in the start of excitation and checking for thermal downshift of Raman lines. The instrument was set up by a software-controlled calibration procedure using multiple neon emission lines (wavelength calibration), multiple polystyrene Raman bands (laser frequency calibration) and standardised white-light sources (intensity calibration). Spectral manipulations were performed using the *Omniscopy 9* software (Thermo Scientific). The Raman bands of kvačekite appear only in the area 250–40  $\text{cm}^{-1}$ , the observed main bands at 199, 179 and 146  $\text{cm}^{-1}$ , with weak to moderate intensity bands at 127, 102, 87, 68, 57 and 45  $\text{cm}^{-1}$  corresponding very well with Raman bands of synthetic NiSbSe (Fig. 3). Strong bands in the area 250–120  $\text{cm}^{-1}$  and medium intensity bands in the range 120–70  $\text{cm}^{-1}$  can be assigned to stretching and bending vibrations of Sb(Ni)–Se bonds. Weak Raman bands below 70  $\text{cm}^{-1}$  should be connected with external modes – translations and librations (Škřácha *et al.*, 2014; Sejkora *et al.*, 2018).

### X-ray diffraction data

The small size of natural kvačekite prevented its extraction and direct investigation by means of X-ray diffraction. Therefore,

**Figure 3.** Raman spectra of kvačekite from Bukov and synthetic NiSbSe.



powder X-ray diffraction data were collected on the synthetic phase NiSbSe at room temperature using a Bruker D8 Advance diffractometer equipped with a solid-state LynxEye detector and secondary monochromator producing CuK $\alpha$  radiation, housed at the Department of Mineralogy and Petrology, National Museum, Prague, Czech Republic. The instrument was operating at 40 kV and 40 mA. In order to minimise the background, the powder was placed on the surface of a flat silicon wafer. The powder pattern was collected in the Bragg–Brentano geometry in the range 3–75°2 $\theta$ , step size 0.01° and counting time of 20 s per step. The positions and intensities of diffractions were found and refined using the Pearson VII profile-shape function of the ZDS program package (Ondruš, 1993). The obtained experimental data correspond well with the powder X-ray diffraction pattern (Table 3) calculated using the software PowderCell2.3 (Kraus and Nolze, 1996) on the basis of our structural model of NiSbSe. The unit-cell parameters for cubic space group  $P2_13$  (# 198) were refined by the least-squares program of Burnham (1962) as follows:  $a = 6.09013(13)$  Å,  $V = 225.881(15)$  Å<sup>3</sup> and  $Z = 4$ . The refined unit-cell parameters agree very well with data  $a = 6.0868(6)$  Å (Foecker and Jeitschko, 2001) and  $a = 6.090(3)$  Å (Hulliger, 1963) given for synthetic NiSbSe.

### Crystal structure

The source data for Rietveld refinement of the synthetic phase NiSbSe were collected at room temperature using a Bruker D8 Advance diffractometer equipped with LynxEye XE detector and CuK $\alpha$  radiation (Czech Geological Survey, Prague). The instrument was operated at 40 kV and 30 mA. In order to minimise the background, the powder was placed on the surface of a flat silicon wafer. The powder pattern was collected in the Bragg–Brentano geometry in the range 10–140°2 $\theta$ , step 0.015°

**Table 3.** Experimental powder X-ray diffraction data for the synthetic analogue of kvačekite (NiSbSe).

Synthetic NiSbSe						Calculated	
$l_{obs.}$	$d_{obs.}$	$d_{calc.}$	$h$	$k$	$l$	$l_{calc.}$	$d_{calc.}$
3.8	4.3087	4.3064	1	1	0	3.6	4.3040
2.6	3.5174	3.5161	1	1	1	2.5	3.5142
<b>11.2</b>	<b>3.0458</b>	3.0451	2	0	0	13.9	3.0434
<b>100.0</b>	<b>2.7242</b>	2.7236	2	0	1	6.9	2.7221
		2.7236	2	1	0	100.0	2.7221
<b>70.7</b>	<b>2.4867</b>	2.4863	2	1	1	79.8	2.4849
6.4	2.1533	2.1532	2	2	0	10.3	2.1520
1.3	1.9258	1.9259	3	0	1	2.0	1.9248
<b>39.4</b>	<b>1.8632</b>	1.8362	3	1	1	55.2	1.8352
3.0	1.7582	1.7581	2	2	2	4.9	1.7571
16.0	1.6891	1.6891	3	0	2	22.5	1.6882
		1.6891	3	2	0	0.9	1.6882
<b>29.1</b>	<b>1.6277</b>	1.6277	3	2	1	21.6	1.6268
		1.6277	3	1	2	21.7	1.6268
7.0	1.5225	1.5225	4	0	0	8.2	1.5217
0.9	1.4353	1.4355	4	1	1	0.9	1.4347
		1.4355	3	3	0	0.9	1.4347
2.1	1.3617	1.3618	4	0	2	2.0	1.3611
		1.3618	4	2	0	2.0	1.3611
<b>12.7</b>	<b>1.3290</b>	1.3290	4	2	1	21.7	1.3283
4.8	1.2984	1.2984	3	3	2	9.3	1.2977

Intensity and  $d_{hkl}$  (in Å) were calculated using the software PowderCell2.3 (Kraus and Nolze, 1996) on the basis of our refined structural model. Only reflections with  $l_{calc.} > 0.5$  are listed. The six strongest reflections are given in bold.

and counting time of 1.4 s per step. The details of data collection and basic crystallographic facts are given in Table 4.

Rietveld refinement was carried out using the Topas 5 program and involved refinement of unit-cell parameter, atomic coordinates, isotropic size and strain parameters. Isotropic displacement parameters were fixed during the refinement ( $B_{iso} = 0.2$  Å<sup>2</sup>). The structure model proposed by Hulliger (1963) and subsequently by Foecker and Jeitschko (2001) for synthetic NiSbSe was confirmed, the refined coordinates did not deviate more than 0.002 from their starting positions. The refined unit-cell parameter  $a = 6.0902(2)$  Å agrees very well with the data  $a = 6.0868(6)$  Å (Foecker and Jeitschko, 2001) and  $a = 6.090(3)$  Å (Hulliger, 1963) given for synthetic NiSbSe. The refinement converged to  $R_{wp} = 0.056$ ,  $R_B = 0.067$  and the final Rietveld plot is shown in Fig. 4. The atomic positions are summarised in Table 5. The crystallographic information file has been deposited with the Principal Editor of *Mineralogical Magazine* and is available as Supplementary material (see below).

Synthetic NiSbSe crystallises in the cubic space group  $P2_13$  and has the ullmannite type structure. It can be considered as a ternary ordered variant of the pyrite-type structure  $MX_2$  ( $Pa\bar{3}$ ), where Sb and Se atoms replace S atoms and are ordered at two independent crystallographic positions X and Y. Consequently, the symmetry is lowered from  $Pa\bar{3}$  (pyrite type) to  $P2_13$  (ullmannite type). Derivation of the kvačekite crystal structure from the pyrite-type and corresponding group–subgroup relation is shown in Fig. 5. The disordered (i.e. pyrite-type) structure model with the Sb/Se mixed site has been also tested in the Rietveld refinement. As indicated in Fig. 6, this structured model yields significantly worse profile agreement factors and cannot fit all observed reflections in the powder diffraction pattern of synthetic NiSbSe. Therefore, the disordered pyrite-type structure can be excluded.

Another ordering of anion atoms occurs in the cobaltite-type structure (CoAsS), which shows orthorhombic symmetry ( $Pca2_1$ ). No indication of peak splitting indicating orthorhombic symmetry have been observed for the synthetic analogue of kvačekite.

The crystal structure of kvačekite is formed by corner-sharing [NiSb<sub>3</sub>Se<sub>3</sub>] octahedra (Fig. 7). There are three Ni octahedra sharing every anion. The Sb and Se atoms form covalent pairs (i.e. dumbbells), with bonding distance of 2.665 Å. A similar bonding

**Table 4.** Powder diffraction data collection and Rietveld analysis of a synthetic analogue of kvačekite, NiSbSe.

Crystal data	
Space group	$P2_13$ (198)
Unit-cell content	NiSbSe, $Z = 4$
Unit-cell parameter (Å)	$a = 6.0902(2)$
Unit-cell volume (Å <sup>3</sup> )	225.89(2)
<b>Data collection</b>	
Radiation type, source	X-ray, CuK $\alpha$
Generator settings	40 kV, 30 mA
Range in 2 $\theta$ (°)	15–140
Step size (°)	0.015
<b>Rietveld analysis</b>	
No. of reflections	95
No. of structural parameters	4
No. of profile parameters	2
$R_{Bragg}$	0.067
$R_p$	0.041
$R_{wp}$	0.056
Weighting scheme	1/ $y_o$

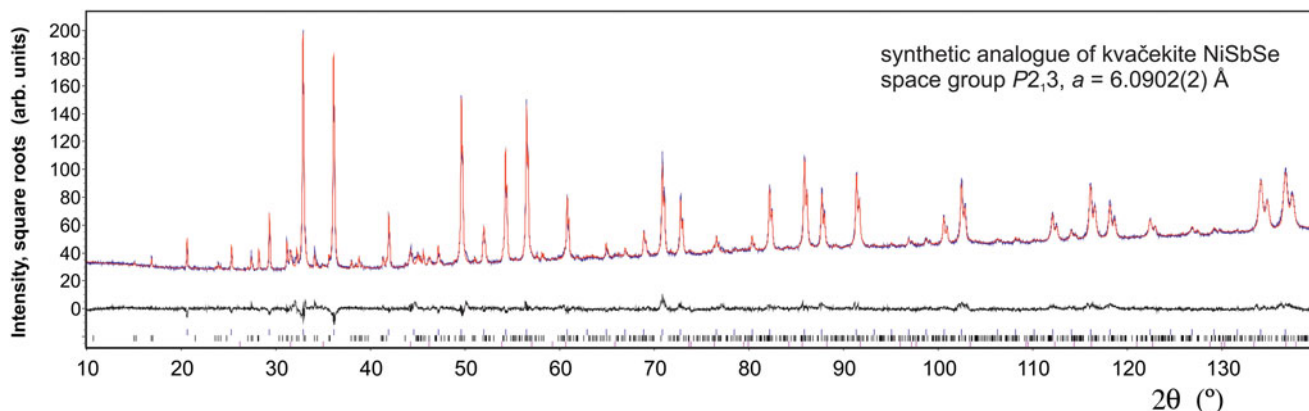


**Figure 4.** Rietveld plot of synthetic analogue of kvačekite, NiSbSe. The refinement reveals 6 and 3 wt.% of  $\text{Sb}_2\text{Se}_3$  and NiSb, respectively, as impurities.

**Table 5.** Atomic fractional coordinates and isotropic displacement parameters in synthetic NiSbSe.

Site	Wyckoff letter.	x	y	z	$B_{\text{iso}}$ ( $\text{Å}^2$ ) <sup>a</sup>
Ni	4a	0.9894(4)	0.9894(4)	0.9894(4)	0.2
Sb	4a	0.6278(2)	0.6278(2)	0.6278(2)	0.2
Se	4a	0.3753(2)	0.3753(2)	0.3753(2)	0.2

<sup>a</sup>Isotropic displacement parameters were fixed during the refinement.

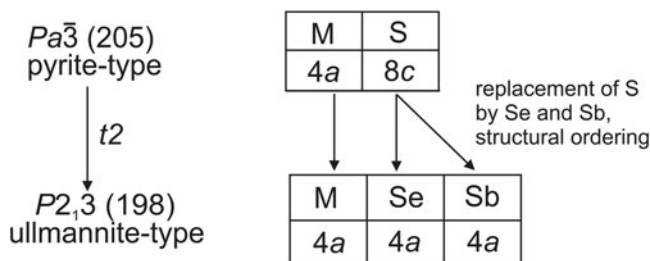


**Figure 5.** The group-subgroup relation ( $Pa\bar{3} \rightarrow P2_13$ ) for the pyrite-type and kvačekite crystal structure showing the splitting of the Wyckoff positions during the reduction of the symmetry (loss of the inversion centre in  $Pa\bar{3}$  space group).

distance of 2.636 Å in Sb–Se covalent pairs was observed in milotaite, PdSbSe (Paar *et al.*, 2005). This is slightly longer than observed Ni–Se and Ni–Sb distances of 2.469(3) and 2.579(3) Å, respectively. Considering Ni–Se distances, slightly longer NiSe separations of 2.503 Å were observed in synthetic NiSe (Unoki *et al.*, 2021), an analogue of sederholmite, which adopts a nickeline-type structure. Ullmannite shows a Ni–Sb distance of 2.563 Å (Foecker and Jeitschko, 2001) which can be compared with the Ni–Sb separations in the kvačekite structure (2.579(3) Å). In addition to ullmannite, the most closely related mineral species is milotaite, PdSbSe (Paar *et al.*, 2005).

### Electron back-scattered diffraction

The structural correlation between the synthetic NiSbSe and the natural kvačekite was confirmed by electron back-scattered diffraction (EBSD). For that purpose, we used a TESCAN Mira 3GMU scanning electron microscope combined with EBSD system Symmetry (Oxford Instruments). The natural sample surface was re-polished with colloidal silica (OP-U) for 20 min to remove an amorphised

layer formed due to standard diamond polishing. The EBSD patterns were collected and processed using the proprietary software *AZtec 6.0* (Oxford Instruments). The Kikuchi patterns obtained from the natural material (35 measurements on different spots on five grains of natural kvačekite) were found to match the patterns generated from our refined structural model for synthetic NiSbSe (Fig. 8). The Kikuchi bands (11, containing 48 reflectors) were detected using the optimised accuracy indexing mode, using band edges, with a Hough resolution of 65. The values of the mean angular deviation (MAD; goodness-of-fit in the solution) between the calculated and measured Kikuchi bands range between 0.11° and 0.36°. These values hence reveal a very good match; mean angular deviations <1° are considered as indicators of an acceptable fit.

### Mineralogy of the associated selenides

A detailed investigation of the selenides associated with kvačekite was undertaken using the same electron microprobe and under the same analytical conditions and correction procedures as previously given for kvačekite.

### Berzelianite

Berzelianite belongs among the most abundant selenides within the samples studied. It occurs as anhedral grains up to 1 cm in size in calcite gangue in association with other selenides. In reflected light it is greenish blue and isotropic.

The chemical composition of berzelianite (Table 6) is relatively uniform and is close to the ideal formula  $\text{Cu}_{2-x}\text{Se}$  (with  $x \approx 0.18$ ). In addition to the main cation (Cu), minor contents of Ag (up to 0.004 apfu), Co (up to 0.031 apfu) and Ni (up to 0.020 apfu) were found, Co and Ni may be an effect of sub-microscopic inclusions of nickeltyrrellite. In the anion part, the range of  $\text{SSe}_{-1}$  substitution is limited to 0.26 apfu S. The mean composition of berzelianite (calculated from 69 point analyses on the basis of 1 Se+S apfu) is  $(\text{Cu}_{1.81}\text{Co}_{0.01})_{\Sigma 1.82}(\text{Se}_{0.89}\text{S}_{0.11})_{\Sigma 1.00}$ .

### Nickeltyrrellite–tyrrellite solid solution

Minerals of the nickeltyrrellite–tyrrellite solid solution are abundant in the association studied. They form euhedral grains (metacrysts) up to 300 μm in size (Fig. 9a) and groups of crystals up to 2 mm in length (Fig. 9b), both enclosed in berzelianite. More

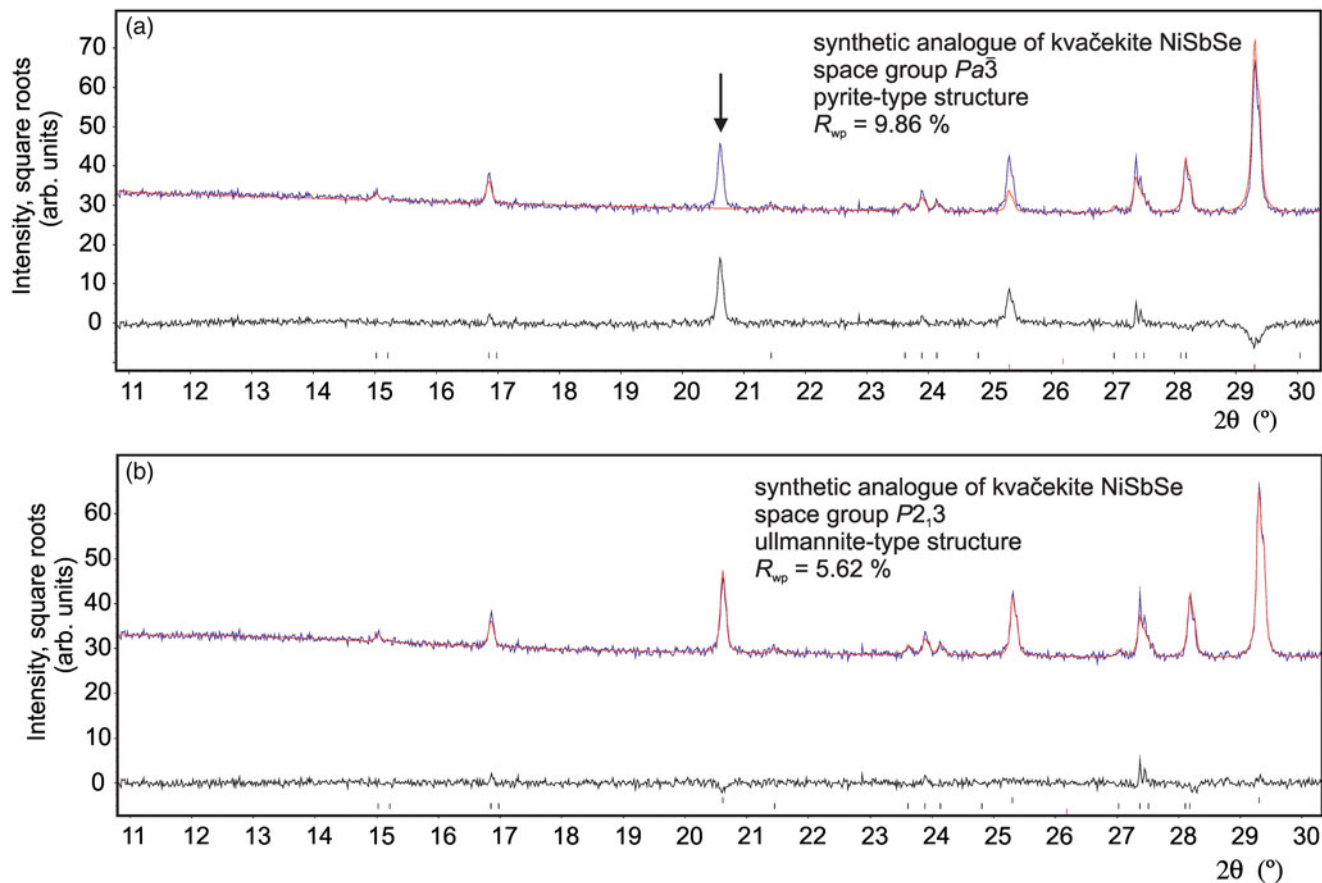


**Figure 6.** Details of the Rietveld refinement of the synthetic analogue of kvačekite NiSbSe using the (a) pyrite and (b) ullmannite structure models. Only the ullmannite structure model is able to fit all of the observed reflection. The unfitted reflection is indicated by an arrow.

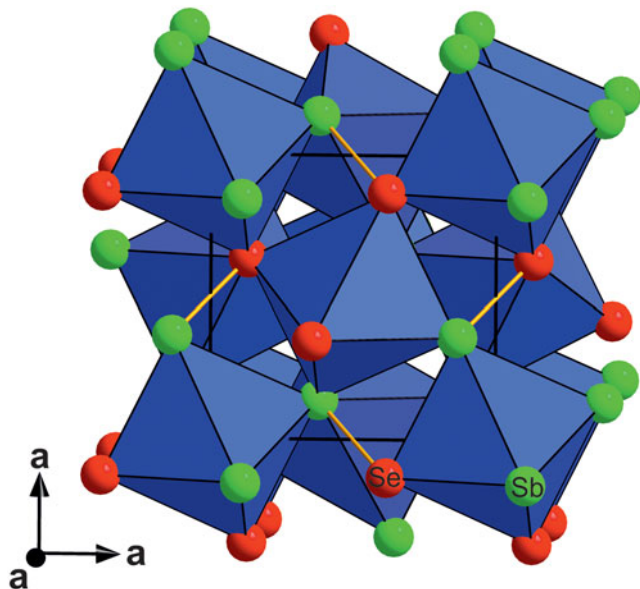


**Figure 7.** Crystal structure of synthetic analogue of kvačekite, NiSbSe, showing the corner-sharing [NiSb<sub>3</sub>Se<sub>3</sub>] octahedrons (in blue). Note the Sb-Se anion pairs. Drawn using *Diamond* (Crystal Impact, 2014).

rarely, they occur as anhedral aggregates up to 800  $\mu\text{m}$  in size in calcite gangue without other selenides (Fig. 9c). In reflected light they are yellowish brown and isotropic.

The chemical composition of the minerals studied corresponds to the formulae  $\text{Cu}(\text{Ni},\text{Co})_2\text{Se}_4$ – $\text{Cu}(\text{Co},\text{Ni})_2\text{Se}_4$  (Förster *et al.*, 2019). The determined representation of  $\text{CoNi}_{-1}$  substitution (Fig. 10) indicates the presence nickeltyrrellite with Ni contents in the wide range of 1.08–2.43 apfu and on the other hand tyrrellite, where Co contents (1.04–1.29 apfu) only slightly prevail over Ni (0.83–1.29 apfu). A wide extent of  $\text{CoNi}_{-1}$  substitution was observed even within individual grains, e.g. from 0.96 to 2.43 apfu Ni in a single grain of 40  $\mu\text{m}$  size. For both minerals, the majority of measured Cu contents (0.55–1.06 apfu) is too low to completely fill the Cu position. It is likely that other cations (Co and/or Ni) have entered this position; a similar situation was described for part of nickeltyrrellite grains from El Dragón by Förster *et al.* (2019). The range of  $\text{SSe}_{-1}$  substitution in nickeltyrrellite (0.01–0.25 apfu S) is close to that of tyrrellite (0.02–0.34 apfu). Representative compositions of minerals of the nickeltyrrellite–tyrrellite solid solutions and the corresponding empirical formulae are given in Table 7.

#### Clausthalite

Clausthalite is a rarer phase, it forms anhedral grains up to 300  $\mu\text{m}$  in size in nickeltyrrellite–tyrrellite and partly replaces earlier berzelianite (Fig. 9d). In reflected light, it is isotropic and has a white colour.

Clausthalite contains, in addition to Pb and Se (Table 6), minor contents of Cu (up to 0.05 apfu) and Co, Ni (both up to



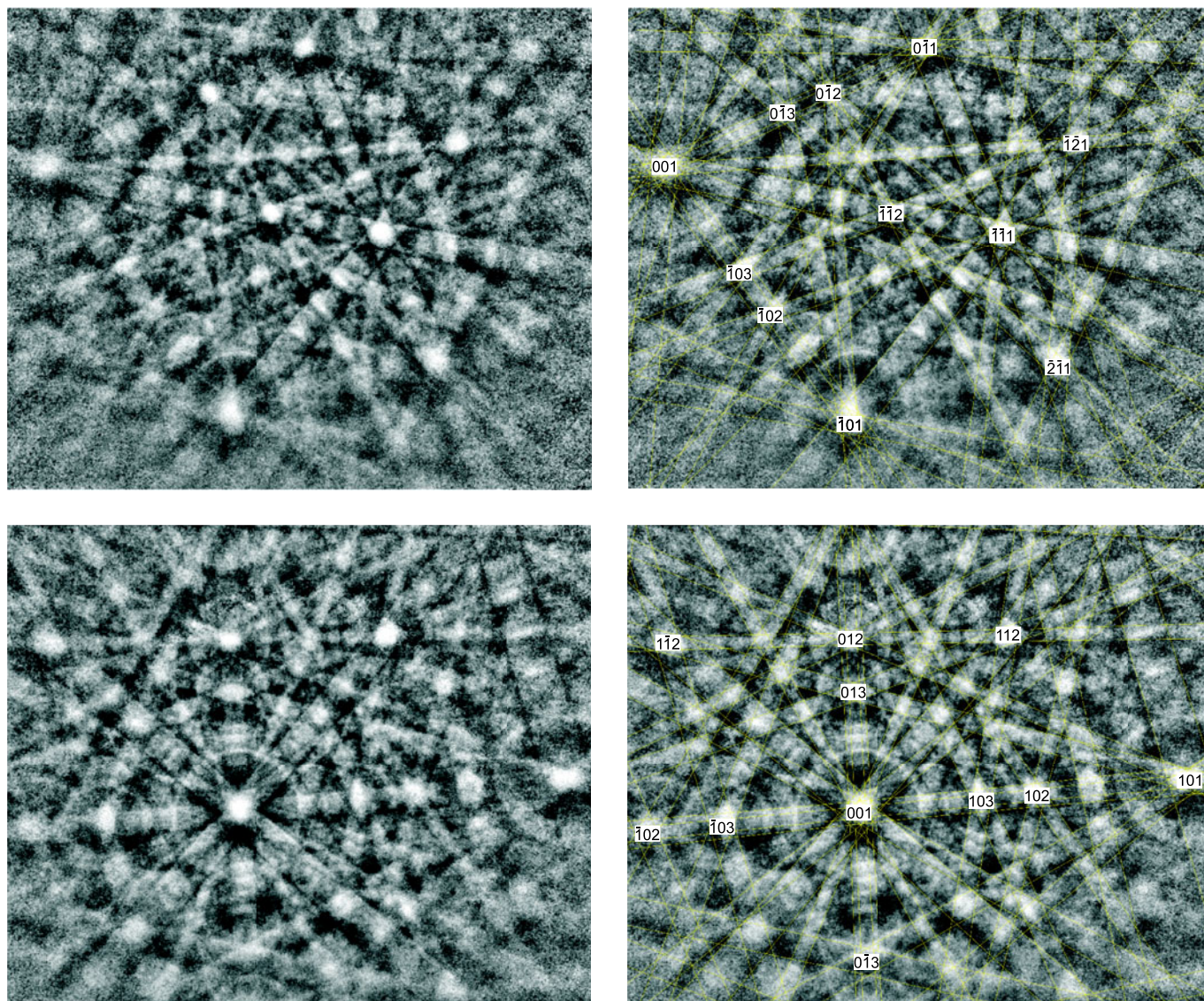


Figure 8. Examples of EBSD images of natural kvačekite; in the right pane, the Kikuchi bands are indexed.

0.02 apfu) and is S-free. Its empirical formula (mean of 23 point analyses on the basis of 2 apfu) is  $(\text{Pb}_{0.97}\text{Cu}_{0.02}\text{Ni}_{0.01}\text{Co}_{0.01})_{\Sigma 1.01}\text{Se}_{0.99}$ .

**Eucairite**

Rare eucairite occurs as anhedral grains up to 100 μm in size and partly replaces earlier berzelianite (Fig. 9e), usually in association with clausthalite and nickeltyrrellite–tyrrellite.

Tiny veinlets of gold (with up to 17 wt.% Ag and 5 wt.% Hg) in eucairite grains were observed only occasionally. In reflected light, eucairite is brown and strongly anisotropic in blue green – blue grey rotation tints.

Its chemical composition (Table 6) is close to the ideal formula  $\text{CuAgSe}$ ; only minor contents of Ni, Co (both up to 0.016 apfu) and Cd (up to 0.004 apfu) were determined. The mean composition of eucairite (calculated from 17 point analyses on the basis of 3 apfu) is  $\text{Ag}_{1.00}\text{Cu}_{1.02}\text{Co}_{0.01}\text{Ni}_{0.01}\text{Se}_{0.96}$ .

**Hakite-(Zn) and hakite-(Cd)**

Hakite forms anhedral grains up to 100 μm in size in berzelianite (Fig. 9f) and nickeltyrrellite–tyrrellite, locally in intergrowths with kvačekite and clausthalite. Hakite replaces

Table 6. EPMA chemical data (wt.%) for berzelianite, clausthalite and eucairite.

Constituent	Berzelianite (n = 69)		Clausthalite (n = 23)		Eucairite (n = 17)	
	Mean	Range	Mean	Range	Mean	Range
Ag	0.11	0.00–0.25	0.00		43.32	42.34–43.96
Cu	61.10	58.70–63.41	0.42	0.00–1.25	26.48	25.61–26.94
Cd	0.00		0.00		0.11	0.00–0.19
Pb	0.00		71.58	70.28–72.33	0.00	
Ni	0.10	0.00–0.61	0.16	0.00–0.45	0.20	0.05–0.37
Co	0.19	0.00–0.94	0.11	0.00–0.32	0.15	0.00–0.38
Se	37.34	31.89–40.83	27.78	27.37–28.16	30.50	30.18–30.97
S	1.83	0.00–4.56	0.00		0.00	
Total	100.67		100.05		100.46	



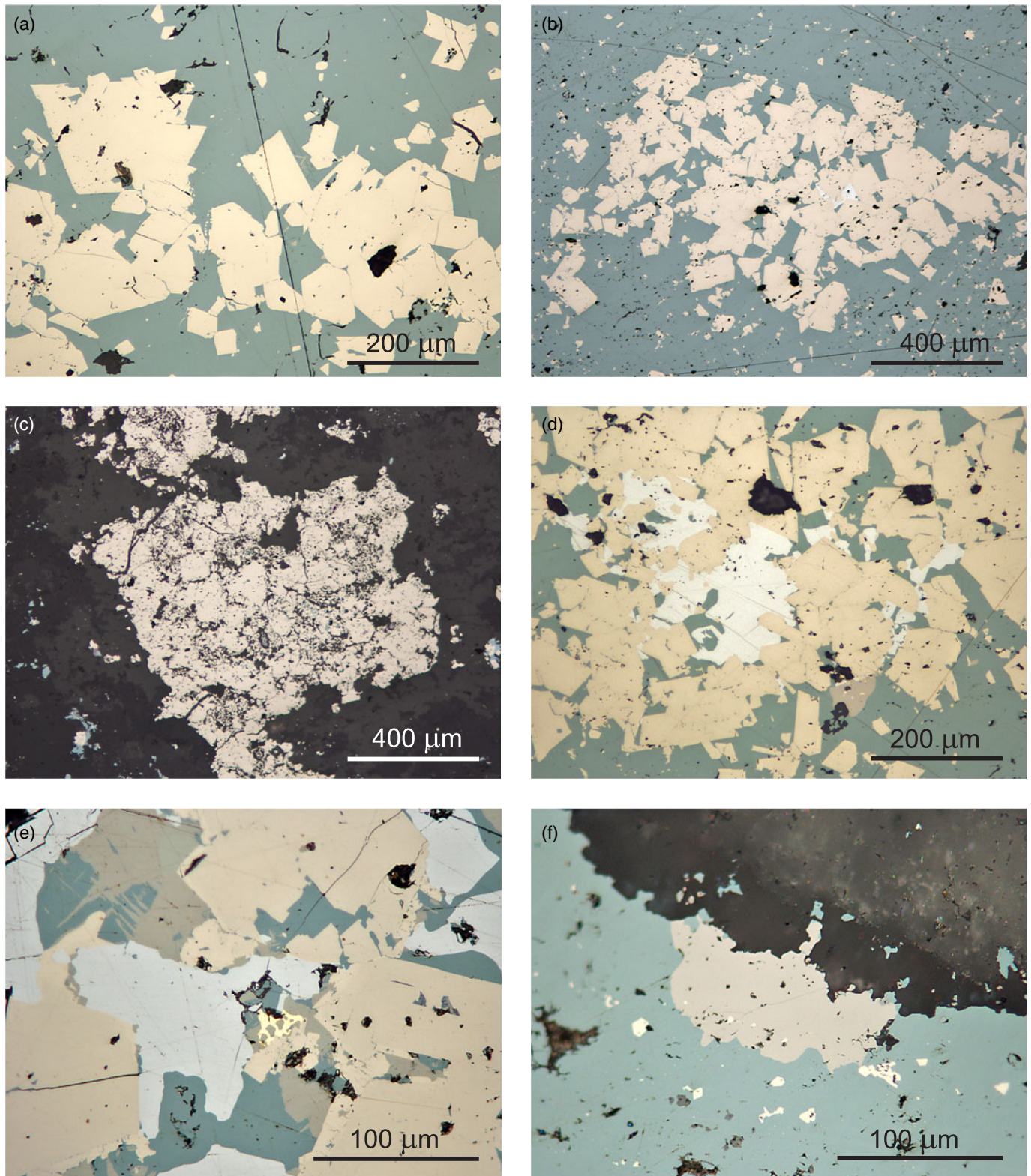


**Figure 9.** Reflected light images of selenides in association with kvačekite from Bukov: (a) euhedral nicketyrrellite–tyrrellite grains (yellowish brown) in berzelianite (greenish blue); (b) groups of nicketyrrellite–tyrrellite grains (yellowish brown) with tiny clausthalite (white) in berzelianite (greenish blue); (c) anhedral nicketyrrellite–tyrrellite aggregates in calcite; (d) clausthalite grains (white) in nicketyrrellite–tyrrellite (yellowish brown) and berzelianite (greenish blue) with tiny hakite-(Zn) (brownish); (e) eucairite grains (brown) with tiny gold veinlets (yellow) in clausthalite (white), berzelianite (greenish blue) and nicketyrrellite–tyrrellite (yellowish brown); (f) hakite-(Zn) grain (brownish) in berzelianite (greenish blue) with tiny nicketyrrellite–tyrrellite inclusions (yellowish brown).



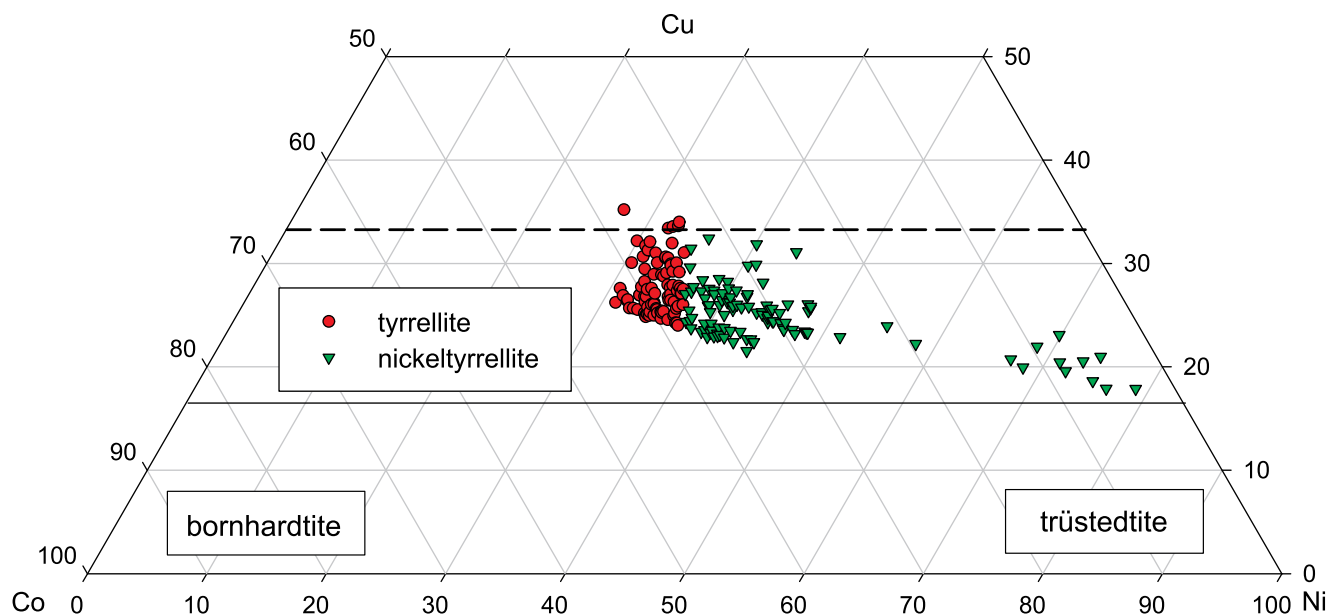


Figure 10. Chemical composition of members of the tyrrellite–nickeltyrrellite series from Bukov in part of the ternary Cu–Co–Ni (at. units) plot. Dashed line corresponds to ideal  $\text{Cu}(\text{Ni},\text{Co})_2\text{Se}_4$  composition.

Table 7. Representative EPMA chemical data (wt.%) and atomic proportions for nickeltyrrellite and tyrrellite.

	Nickeltyrrellite								Tyrrellite				
Ni	13.16	13.65	14.10	14.27	14.70	17.41	26.13	29.28	9.94	11.61	11.27	12.37	13.57
Co	12.80	12.15	13.58	13.92	13.07	10.07	2.66	1.23	13.68	15.74	15.52	12.76	14.03
Cu	12.87	13.38	11.47	9.48	9.22	9.03	9.35	7.19	13.85	11.26	10.29	13.98	9.42
Se	62.18	61.74	60.54	62.18	62.43	62.86	62.65	63.60	61.75	60.22	61.28	61.83	63.41
S	0.74	0.56	1.71	0.43	0.43	0.17	0.05	0.04	1.04	2.32	1.07	0.82	0.15
Total	101.75	101.48	101.40	100.28	99.85	99.54	100.84	101.34	100.26	101.15	99.43	101.76	100.58
Coefficients of empirical formulae calculated on the basis of 7 apfu													
Ni	1.079	1.123	1.143	1.190	1.233	1.471	2.175	2.425	0.827	0.937	0.942	1.013	1.135
Co	1.045	0.996	1.096	1.157	1.092	0.848	0.221	0.101	1.133	1.266	1.292	1.041	1.169
Cu	0.975	1.017	0.859	0.731	0.715	0.705	0.719	0.550	1.064	0.840	0.794	1.058	0.728
Se	3.790	3.778	3.648	3.857	3.894	3.950	3.878	3.917	3.818	3.614	3.808	3.765	3.944
S	0.111	0.084	0.254	0.066	0.066	0.026	0.008	0.006	0.158	0.343	0.164	0.123	0.023

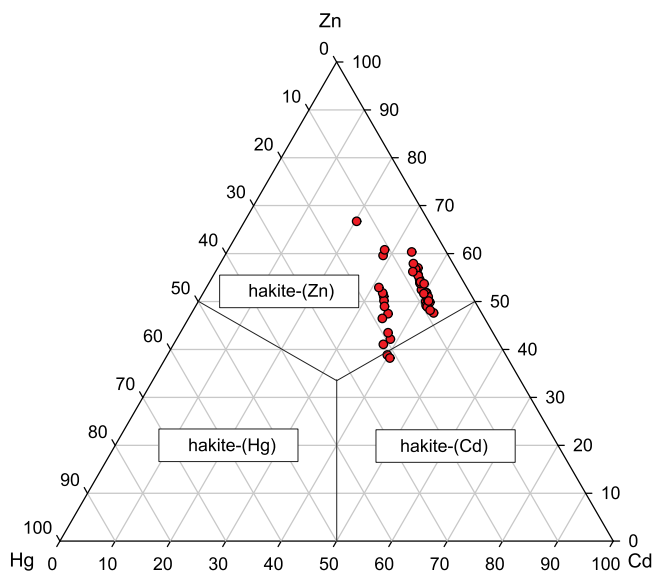


Figure 11. Chemical composition of members of the hakite series in the ternary Zn–Hg–Cd (at. units) plot; non-dominant elements Ni (up to 0.19 apfu), Co (up to 0.16 apfu) and calculated  $\text{Cu}^{2+}$  (up to 0.60 apfu) are omitted.

earlier berzelianite and clausthalite and can contain relics of these minerals and of nickeltyrrellite. In reflected light it is brownish and isotropic.

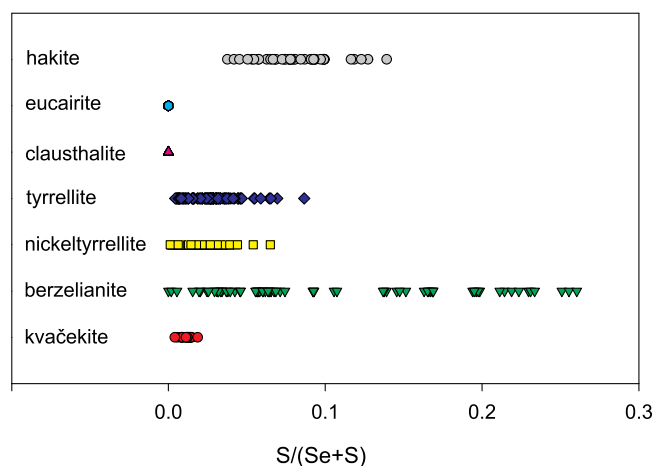
According to the nomenclature scheme of minerals of the tetrahedrite group (Biagioni *et al.*, 2020) the studied minerals correspond to hakite-(Zn) and two point analyses to hakite-(Cd), both with regular minor Hg contents (Fig. 11). Both minerals were recently defined as new minerals on samples from the Příbram uranium ore district (Czech Republic) by Sejkora *et al.* (2024). The trigonal position of both studied members from Bukov is predominantly occupied by Cu, with minor amounts of Ag (up to 0.60 apfu). Zinc, and in the case of two point analyses Cd, are dominant  $\text{Me}^{2+}$  elements; there are two trends in minor contents of Hg (Fig. 11) – approximately 0.13 apfu and in the range 0.19–0.39 apfu. The calculated  $\text{Cu}^{2+}$  contents reach up to 0.60 apfu. Locally minor contents of Ni and Co were observed, reaching up to 0.19 and 0.16 apfu, respectively. The studied hakites are pure Sb members and the range of  $\text{SSe}_{-1}$  substitution is limited to 1.70 apfu S. Representative chemical analyses of hakite-series minerals and the corresponding empirical formulae are given in Table 8.

**Table 8.** Representative EPMA chemical data (wt.%) and atomic proportions for hakite-(Zn) and hakite-(Cd).

	Hakite-(Zn)						Hakite-(Cd)																		
	Ag	Cd	Ni	Co	Zn	Hg	Cu	Sb	Se	S	Total	Ag	Cd	Ni	Co	Zn	Hg	Cu	Sb	Se	S	Total			
Ag	0.88	0.67	0.71	1.77	0.21	0.00	0.64	0.20	2.78	0.19	100.38	0.56	0.83	3.61	3.58	0.00	0.18	0.00	0.12	0.47	0.00	0.00	0.00	0.18	
Cd	3.33	3.62	3.41	3.30	2.85	3.17	3.45	3.48	1.51	2.58	20.86	3.61	3.58	0.00	0.00	0.05	0.00	0.09	0.41	0.00	0.00	0.00	0.00	0.12	
Ni	0.21	0.00	0.00	0.06	0.00	0.00	0.00	0.12	0.47	0.00	40.33	0.00	0.18	0.00	0.00	0.00	0.00	0.04	0.186	0.000	0.000	0.000	0.000	0.069	
Co	0.17	0.00	0.00	0.00	0.00	0.05	0.00	0.09	0.41	0.00	20.91	0.00	0.069	0.000	0.019	0.000	0.034	0.162	0.000	0.000	0.000	0.000	0.000	0.046	
Zn	2.33	2.29	2.34	2.72	2.99	2.90	2.17	2.34	2.89	3.22	21.44	2.05	1.96	0.00	0.00	0.00	0.00	0.00	0.00	0.00	0.00	0.00	0.00	0.00	0.00
Hg	1.19	1.28	1.35	1.20	0.95	1.06	3.41	3.13	1.73	1.78	21.47	3.47	3.35	0.00	0.00	0.00	0.00	0.00	0.00	0.00	0.00	0.00	0.00	0.00	0.00
Cu	29.70	27.63	28.33	28.20	30.57	28.42	28.22	28.16	25.90	30.40	21.59	28.63	27.87	0.00	0.00	0.00	0.00	0.00	0.00	0.00	0.00	0.00	0.00	0.00	0.00
Sb	20.86	21.04	20.91	21.44	21.47	21.59	21.01	21.74	21.26	22.20	21.01	21.08	21.59	0.00	0.00	0.00	0.00	0.00	0.00	0.00	0.00	0.00	0.00	0.00	0.00
Se	40.33	40.55	41.08	39.79	39.33	39.02	40.98	40.69	41.19	38.69	40.98	41.16	41.08	0.00	0.00	0.00	0.00	0.00	0.00	0.00	0.00	0.00	0.00	0.00	0.00
S	1.38	1.20	1.02	1.62	2.24	2.13	0.65	1.18	0.89	2.54	0.65	0.73	0.79	0.00	0.00	0.00	0.00	0.00	0.00	0.00	0.00	0.00	0.00	0.00	0.00
Total	100.38	98.28	99.15	100.10	100.61	98.34	100.53	101.13	99.03	101.60	100.53	101.29	101.35												

Coefficients of empirical formulae calculated on the basis of 16 Me apfu

Ag	0.180	0.145	0.151	0.368	0.042	0.000	0.135	0.042	0.598	0.038	0.117	0.174
Cd	0.654	0.750	0.696	0.658	0.552	0.642	0.698	0.698	0.312	0.494	0.724	0.721
Ni	0.079	0.000	0.000	0.023	0.000	0.000	0.000	0.046	0.186	0.000	0.000	0.069
Co	0.064	0.000	0.000	0.000	0.000	0.019	0.000	0.034	0.162	0.000	0.000	0.046
Zn	0.787	0.815	0.822	0.932	0.995	1.009	0.755	0.807	1.026	1.060	0.707	0.678
Hg	0.131	0.149	0.154	0.134	0.103	0.120	0.387	0.352	0.200	0.191	0.390	0.378
Cu	10.321	10.120	10.234	9.941	10.470	10.175	10.100	9.993	9.462	10.294	10.158	9.922
Sb	3.784	4.022	3.942	3.945	3.838	4.034	3.925	4.027	4.054	3.924	3.904	4.012
Se	11.279	11.953	11.943	11.288	10.840	11.243	11.804	11.621	12.110	10.543	11.753	11.770
S	0.950	0.871	0.730	1.132	1.520	1.511	0.461	0.830	0.644	1.705	0.513	0.557

**Figure 12.** Range of S/(Se+S) substitution of described selenides from Bukov (at. units).

## Conclusions

Kvačekite is a new ternary phase in the Ni–Sb–Se system and a member of the cobaltite group. It does not correspond to any valid or invalid unnamed mineral (Smith and Nickel, 2007; <http://cnmnc.units.it/>). Its identity with synthetic cubic NiSbSe (Hulliger, 1963; Foecker and Jeitschko, 2001) was confirmed by a study of their chemical composition, reflectance measurements, Raman spectroscopy and electron back-scattered diffraction (EBSD) measurements on the natural sample.

Kvačekite occurs in a Ni–Co–Cu rich mineral association, which also represents the second world occurrence for nickelytyrrellite (Förster et al., 2019), hakite-(Zn) and hakite-(Cd) (Sejkora et al., 2024). This association hosted by a calcite gangue exhibits a limited range of SSe<sub>-1</sub> substitution (Fig. 12). The selenide mineralisation studied originated from Ni–Co–Cu-bearing fluids at temperatures above 112°C (absence of umangite, Chakrabarti and

Laughlin, 1981) with neutral-to-weakly-alkaline character, high oxygen fugacity and a Se<sub>2</sub>/S<sub>2</sub> fugacity ratio greater than unity.

**Acknowledgements.** The helpful comments of anonymous reviewer, Panagiotis Voudouris, Peter Leverett, Associate Editor Ian Graham and Principal Editor Stuart Mills are greatly appreciated. The study was financially supported by the Ministry of Culture of the Czech Republic (long-term project DKRVO 2024-2028/1.II.a; National Museum, 00023272) and by the Grant Agency of the Czech Republic (project No 22-26485S).

**Supplementary material.** The supplementary material for this article can be found at <https://doi.org/10.1180/mgm.2024.32>.

**Competing interests.** The authors declare none.

## References

- Biagioni C., George L.G., Cook N.J., Makovicky E., Moëlo Y., Pasero M., Sejkora J., Stanley C.J., Welch M.D. and Bosi F. (2020) The tetrahedrite group: Nomenclature and classification. *American Mineralogist*, **105**, 109–122.
- Burnham C.W. (1962) Lattice constant refinement. *Carnegie Institute Washington Yearbook*, **61**, 132–135.
- Chakrabarti D.J. and Laughlin D.E. (1981) The Cu–Se (copper–selenium) system. *Bulletin of Alloy Phase Diagrams*, **2**, 305–315.
- Crystal Impact (2014) *Diamond – Crystal and Molecular Structure Visualization*. Dr. H. Putz & Dr. K. Brandenburg GbR, Kreuzherrenstr. 102, 53227 Bonn, Germany, <http://www.crystalimpact.com/diamond>.
- Foecker A.J. and Jeitschko W. (2001) The atomic order of the pnictogen and chalcogen atoms in equiatomic ternary compounds T<sub>3</sub>PnCh (T= Ni, Pd; Pn= P, As, Sb; Ch= S, Se, Te). *Journal of Solid State Chemistry*, **162**, 69–78.
- Förster H.J., Ma C., Grundmann G., Bindi L. and Stanley C.J. (2019) Nickelytyrrellite, CuNi<sub>2</sub>Se<sub>4</sub>, a new member of the spinel supergroup from El Dragón, Bolivia. *The Canadian Mineralogist*, **57**, 637–646.
- Hulliger F. (1963) New compounds with cobaltite structure. *Nature*, **198**, 382–383.
- Johan Z. and Kvaček M. (1971) La bukovite, Cu<sub>3+x</sub>Tl<sub>2</sub>FeSe<sub>4-x</sub>, une nouvelle espèce minérale. *Bulletin de Minéralogie*, **94**, 529–533.
- Johan Z., Kvaček M. and Picot P. (1978) La sabatierite, un nouveau sélénure de cuivre et de thallium. *Bulletin de Minéralogie*, **101**, 557–560.
- Kraus W. and Nolze G. (1996) POWDER CELL – a program for the representation and manipulation of crystal structures and calculation of the resulting X-ray powder patterns. *Journal of Applied Crystallography*, **29**, 301–303.



- Křibek B., Žák K., Dobeš P., Leichmann J., Pudilová M., René M., Scharm B., Scharmová M., Hájek A., Holeczy D., Hein U.F. and Lehmann B. (2009) The Rožná uranium deposit (Bohemian Massif, Czech Republic): shear zone-hosted, late Variscan and post-Variscan hydrothermal mineralization. *Mineralium Deposita*, **44**, 99–128.
- Křibek B., Kněsl I., Dobeš P., Veselovský F., Pořádek P., Škoda R., Čopjaková R., Leichmann J. and Košek F. (2022) The origin of synchysite-(Ce) and sources of rare earth elements in the Rožná uranium deposit, Czech Republic. *Minerals*, **12**, 690.
- Kvaček M. (1973) Selenides from the uranium deposits of western Moravia, Czechoslovakia - part 1. Berzelianite, umangite, eskebornite. *Acta Universitatis Carolinae, Geologica*, **17**, 23–36.
- Kvaček M. (1979) Selenides from the uranium deposits of western Moravia, Czechoslovakia - part 2. *Acta Universitatis Carolinae, Geologica*, **23**, 15–38.
- Ondruš P. (1993) A computer program for analysis of X-ray powder diffraction patterns. *Materials Science Forum, EPDIC-2, Enchede*, **133–136**, 297–300.
- Paar W.H., Topa D., Makovicky E. and Culetto F. (2005) Milotaitite, PdSbSe, a new palladium mineral species from Předbořice, Czech Republic. *The Canadian Mineralogist*, **43**, 689–694.
- Pauliš P., Dolníček Z., Sejkora J., Pour O., Laufek F., Ulmanová J. and Vymazalová A. (2024) Kvačekite, IMA 2023-095. CNMNC Newsletter 77; *Mineralogical Magazine*, **88**, 203–209. <https://doi.org/10.1180/mgm.2024.5>.
- Pouchou J.L. and Pichoir F. (1985) “PAP” ( $\varphi\rho Z$ ) procedure for improved quantitative microanalysis. Pp. 104–106 in: *Microbeam Analysis* (J.T. Armstrong, editor). San Francisco Press, San Francisco.
- Sejkora J., Buixaderas E., Škacha P. and Plášil J. (2018) Micro-Raman spectroscopy of natural members along CuSbS<sub>2</sub>–CuSbSe<sub>2</sub> join. *Journal of Raman Spectroscopy*, **49**(8), 1364–1372.
- Sejkora J., Biagioni C., Škacha P., Musetti S. and Dolníček Z. (2024) Three new Cd-, Fe- and Zn-dominant members of the hakite series from the Bytíz deposit, uranium and base-metal Příbram ore district, Czech Republic. *Mineralogical Magazine*, **88**, 602–612.
- Škacha P., Buixaderas E., Plášil J., Sejkora J., Goliáš V. and Vlček V. (2014) Permingeatite, Cu<sub>3</sub>SbSe<sub>4</sub>, from Příbram (Czech Republic): description and Raman spectroscopy investigations of the luzonite-subgroup of minerals. *The Canadian Mineralogist*, **52**, 501–511.
- Smith D.G.W. and Nickel E.H. (2007) A system for codification for unnamed minerals: report of the Subcommittee for Unnamed Minerals of the IMA Commission on New Minerals, Nomenclature and Classification. *The Canadian Mineralogist*, **45**, 983–1055.
- Unoki K., Yoshiasa A., Kitahara G., Nishiyama T., Tokuda M., Sugiyama K. and Nakatsuka A. (2021) Crystal structure refinements of stoichiometric Ni<sub>3</sub>Se<sub>2</sub> and NiSe. *Acta Crystallographica*, **C77**, 169–175.
- Warr L.N. (2021) IMA-CNMNC approved mineral symbols. *Mineralogical Magazine*, **85**, 291–320.